Humidity Dependence of Charge Transport through DNA Revealed by Silicon-Based Nanotweezers Manipulation

Christophe Yamahata,* Dominique Collard,† Tetsuya Takekawa,‡ Momoko Kumemura,* Gen Hashiguchi,‡ and Hiroyuki Fujita*

*Institute of Industrial Science, †LIMMS/CNRS-IIS (UMI 2820), the University of Tokyo, Tokyo, Japan; and ‡Faculty of Engineering, Kagawa University, Takamatsu, Japan

ABSTRACT The study of the electrical properties of DNA has aroused increasing interest since the last decade. So far, controversial arguments have been put forward to explain the electrical charge transport through DNA. Our experiments on DNA bundles manipulated with silicon-based actuated tweezers demonstrate undoubtedly that humidity is the main factor affecting the electrical conduction in DNA. We explain the quasi-Ohmic behavior of DNA and the exponential dependence of its conductivity with relative humidity from the adsorption of water on the DNA backbone. We propose a quantitative model that is consistent with previous studies on DNA and other materials, like porous silicon, subjected to different humidity conditions.

INTRODUCTION

DNA has long remained the sole purview of biologists but nanotechnology has since fostered the extensive study of this molecule through numerous other disciplines. In bottom-up nanotechnology, DNA molecule is considered as an interesting engineering material due to its self-assembling capability (1,2). In a top-down approach, the recent achievements in nanometer-scale instrumentation have enabled the micromanipulation of single molecules through the use of magnetic tweezers, optical tweezers, or atomic force microscopy (AFM) (3,4). Biophysicists have thus measured significant mechanical responses of DNA strands interacting with proteins (5). In nanoelectronics, DNA has also been considered as a possible electric nanowire. Although unmodified DNA lacks sufficient conductivity, the electrical properties of DNA are still a current concern (6). Indeed, if DNA is to be used as a building block for molecular electronic devices, the question of conductivity has to be solved.

Several reviews have amassed articles discussing the question of DNA conductivity (6–8). Although many aspects still remained controversial, they have also progressed toward establishing the physical origin of this conductivity. In the frame of our study, we summarize hereafter a nonexhaustive list of the main conclusions obtained from the different works published so far.

The first experiments on DNA conductivity were conducted on few-nanometers-long DNA ropes (9,10) and since then, most of the studies have been carried out by measuring the current flowing through DNA bundles deposited on nanoelectrodes. Only a few authors have used AFM-like methods: H. Watanabe et al. (11) used an AFM and a triple-probe technique in an attempt to observe the semiconductive properties of DNA; an AFM was also used by Cohen et al. (12) to verify the conductivity through DNA bundles.

Cai et al. (13,14) studied the influence of nucleotides arrangement on the global conductivity of DNA. Several groups also reported that poly(dA)-poly(dT) and poly(dG)-poly(dC) have different conductivity characteristics (13,15–17). In an attempt to enhance the conductivity of DNA, Rakitin et al. (18) substituted imino proton of each basepair with a metallic ion. For the same purpose, several authors also studied the conductivity through modified DNA (2,19–23). In particular, an interesting approach was developed by Maruccio et al. (20), who proposed a prototype transistor based on a deoxyguanosine derivative.

Tran et al. (24) studied the effect of temperature on DNA conductivity and also reported the influence of water. The major influence of humidity on DNA conductivity was later discussed by a few other groups (25–28). Their conclusions have led us to consider that the humidity should be a major concern regarding its implication in the other studies which, most often, did not take its effect into account. The recent studies on relative humidity could partially elucidate some of the conflicting theories on DNA conductivity. However, none of the experiments conducted so far could establish a clear relation between DNA conduction caused by humidity and the influence of other dimensional parameters such as DNA length or the bundle diameter.

To address the question of DNA conductivity and the influence of humidity, we used microelectromechanical system (MEMS)-based nanotweezers to handle DNA molecules. We have designed a versatile device that enables the straightforward trapping of DNA between aluminum-coated silicon nanotips by AC dielectrophoresis (21,29), and offers the possibility of simultaneous mechanical stretching and electrical characterization of the captured DNA bundle (4,30,31). A three-dimensional (3D) schematic view of the

Submitted June 22, 2007, and accepted for publication August 23, 2007.

Address reprint requests to Christophe Yamahata, Tel.: 81-3-5452-6249; E-mail: christophe.yamahata@a3.epfl.ch.

Editor: Kathleen B. Hall.

0006-3495/08/01/63/08 $2.00

doi: 10.1529/biophysj.107.115980

device is illustrated in Fig. 1 *a*. The experiments reported in this article were conducted on DNA bundles having different diameters that were suspended in air (see Fig. 1 *b*). The latter point is of particular importance because it ensures the unambiguous measurement of conductivity through DNA itself. Indeed, any parallel current flow through the moisturized surface of the substrate is avoided.

Our results are compared to previous studies and we summarize the hypothesis based on conductivity mediated by adsorbed water. From our tweezers-based experiments, we suggest that 1), DNA has a quasi-Ohmic behavior under constant temperature and humidity conditions; and 2), the exponential dependence of conductivity with the relative humidity could be explained by the change of permittivity arising from water adsorption on the DNA backbone. The formulated theory is relevant with regard to the quantitative data gathered from other studies conducted on DNA in a wet environment.

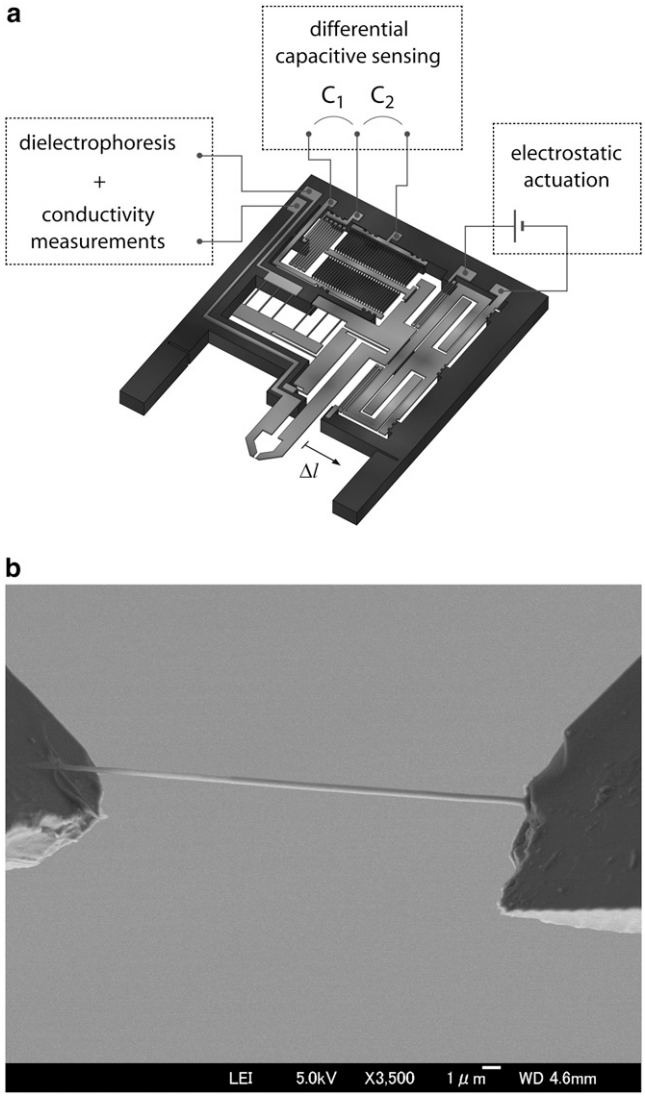

FIGURE 1 3D view of the MEMS silicon device and micrograph of a DNA bundle. (*a*) The MEMS nanotweezers are fabricated using SOI technology. The electrostatic actuator, the differential capacitive sensor and the nanotips are electrically isolated. The displacement, Δl, of the moving tip results in a change of the variable capacitances C_1 and C_2 used for sensing. (*b*) A DNA bundle captured between silicon tips coated with aluminum. On this picture, the bundle has a mean diameter of ~380 nm.

METHODS

Device fabrication

The silicon nanotweezers were fabricated using silicon-on-insulator (SOI) technology. The different fabrication steps are summarized below (30). We started from a SOI substrate having the following characteristics: (100)–oriented, 25-μm-thick silicon active layer/1.5-μm buried oxide insulator/380-μm handling substrate. A thin Si_3N_4 layer was first deposited on the wafer by low pressure chemical vapor deposition and patterned to form rectangular areas along the $\langle 100 \rangle$ direction. The silicon over layer was then etched by deep reactive ion etching. The silicon tips were obtained by the combination of wet anisotropic etching and local oxidation of silicon techniques: A wet oxidation process at 1100°C was used to cover the structured silicon with SiO_2; after removal of the Si_3N_4, a KOH wet anisotropic etching of silicon was performed to obtain $\{111\}$ facets, which eventually made sharp tips. Next, the buried oxide was removed by HF and the backside silicon was structured by deep reactive ion etching. In the last step, a few nanometers thick aluminum film was evaporated on the silicon over layer. This aluminum coating acts as an anchor material to DNA molecules (32,33). A 3D view of the device is illustrated in Fig. 1 *a*.

DNA trapping

A solution of double-stranded λ-DNA (48.5 kbp, 16-μm-long) was obtained from Takara Bio (Shiga, Japan). After dilution in deionized water, a small droplet of the solution was pipetted on a microscope cover glass and placed under a VHX-500 Digital Microscope (Keyence, Osaka, Japan). With the help of a 3D Cartesian stage, the silicon nanotweezers were then approached to the surface of the droplet. By applying a high frequency electric field (40 V_{pk-pk}, 1 MHz, ~20-μm gap) for few seconds, DNA strands were attracted by dielectrophoresis and a bundle of DNA could form at the end of the tips, as shown in the field emission scanning electron microscopy (FESEM) image of Fig. 1 *b*. At the end of the experiments, the DNA rope was simply removed from the tips by blowing air and rinsing with alcohol. The trapping process could be repeated many times, as long as aluminum coating was present on the silicon tips. One should note that all the experiments described in this article were performed on the same silicon device.

The trapping of DNA molecules by dielectrophoresis was pioneered by Washizu et al. (32) and we recently applied this method to demonstrate the isolation and trapping of single molecules of double-stranded DNA in a microfluidic device (34). From our own experience, the binding of double-stranded DNA on gold electrodes was not possible but it could easily be achieved when using aluminum material. The mechanism of DNA/aluminum interaction is still not well understood. A possible explanation for this binding could be that aluminum is an electrochemically active material. For example, while the direct binding of DNA to gold electrodes is not feasible without functionalization of DNA (too weak), it is possible with aluminum (strong) or with platinum electrodes (weaker) (35). For a detailed discussion on the nature of this binding, we refer the reader to the articles of Washizu and co-workers (32,35). Moreover, the works of Wu et al. (36) and Wang and Bard (37) could provide additional explanation. The former authors report different techniques used to investigate the thermodynamics of the binding of aluminum ions to calf thymus DNA. The latter detail the use of aluminum-based films to immobilize both single-stranded and double-stranded DNA. In that case, the binding is due to the interaction of a positively charged metallic film (Al^{3+}) with the phosphate group of DNA.

Electrical measurements

For the experimental data reported later in Fig. 3, the displacement Δl was measured by differential capacitive sensing (4,30,31) ($\Delta C = C_2 - C_1$) with the commercial Capacitive Readout MS3110 (Irvine Sensors, Costa Mesa, CA) connected to the variable comb capacitances C_1 and C_2 (see Fig. 1 *a*).

All the electrical measurements on DNA bundles were performed in a Faraday cage with a 6487 Picoammeter/Voltage source (Keithley Instruments, Cleveland, OH). We observed that the DNA bundle could sometimes cover the tip. This resulted in an effective surface contact larger than the tip/DNA point contact interaction but we did not observe any influence on our measurements. The contact resistance effect can be considered lower than the resistance of the bundle itself. For this reason, the four-point probe measurement method was not required.

For monitored humidity conditions, the experimental setup was placed in a glove box connected to a humidity generator. The latter consisting of a pump supplying ambient air through a gas washing bottle whose flow could be adjusted to control the humidity level in the glove box. The temperature and relative humidity conditions were recorded in real-time with the Temperature/Humidity Datalogger SK-L200TH IIα (Sato Keiryoki, Tokyo, Japan).

Microscopy characterization

After electrical measurements, the diameters of DNA bundles were measured by FESEM imaging with the JSM-7400F microscope (Jeol, Tokyo, Japan).

RESULTS

Ohmic behavior

To verify the quasi-Ohmic behavior of DNA bundles reported in previous studies (8), we have conducted different kinds of experiments to measure the variation of the current I as a function of the applied voltage U (two points measurements method), the influence of the bundle diameter ϕ, and finally an increase Δl of its length l by mechanical stretching. This first set of experiments was performed under a relative humidity $rh = 50 \sim 60\%$ with an ambient temperature $T = 25°C$. Fig. 2 *a*, gives the $I - U$ curves obtained for different bundles (various values of ϕ). As reported in the literature, the current does not vary linearly with the applied voltage (8). As a first approximation, without loss of generality of our analysis, we can nevertheless consider that this behavior is quasi-linear. From Fig. 2 *a*, we extracted $I(U = 10\ \text{V})$ and reported these values versus the diameter ϕ of dried bundles, as measured afterwards by FESEM (see Fig. 1 *b*). The results are reported in Fig. 2 *b*. The curve is a parabolic fit that shows the quadratic dependence $I \propto \phi^2$. With our MEMS device, it was also possible to stretch the DNA bundle and simultaneously measure its conductivity. We conducted such experiment on a thin DNA bundle and the measurements are reproduced in Fig. 3. When interpreting these results, one should consider that the first effect of stretching is to elongate the bundle; but intuitively, we can also suppose that the bundle gets slightly thinner (reduction of S). However, we do not retain this effect as being responsible for the decrease of the current. Indeed, even if S decreases under stretching, the number of DNA strands remains constant in the section. On the other hand, if the reduction of the cross section, ΔS, was significant compared to the increase of length, Δl, the two effects would add up, resulting in a slope different from –1, as observed in Fig. 3: The relative variation of the current, $\Delta I/I$, as a function of the relative elongation of the bundle, $\Delta l/l$, shows that $\Delta I/I = -\Delta l/l$, which means that $I \propto 1/l$. From all these experiments, we can thus conclude that the DNA bundle has a quasi-Ohmic behavior,

$$I = \sigma \frac{S}{l} U, \tag{1}$$

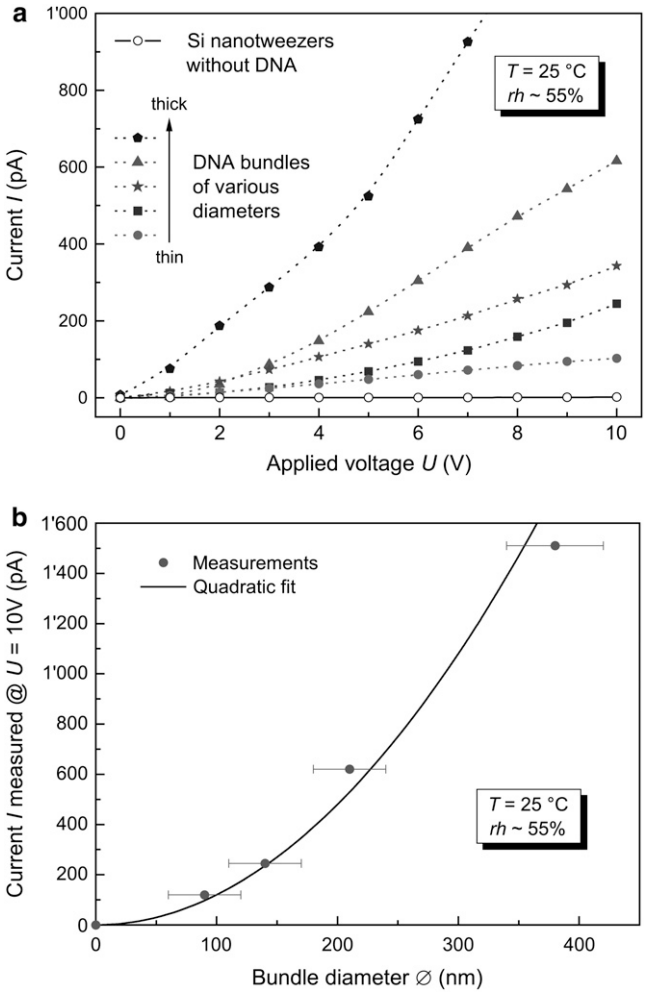

FIGURE 2 Electrical conductivity through DNA bundles. The measurements were performed on different DNA bundles whose diameters ranged from ~100 nm to a few microns. Electrical conductivity data recorded at $T = 25°C$ for $rh = 50 \sim 60\%$. (*a*) Current measurement as a function of the applied DC voltage. The dotted lines are guides for the eye. (*b*) Quadratic dependence of the conductivity with the bundle diameter. After measurement of the stabilized conductivity (reported in *a*), we observed the dried DNA bundles under a FESEM to estimate their diameter ϕ. The curve is a quadratic fit.

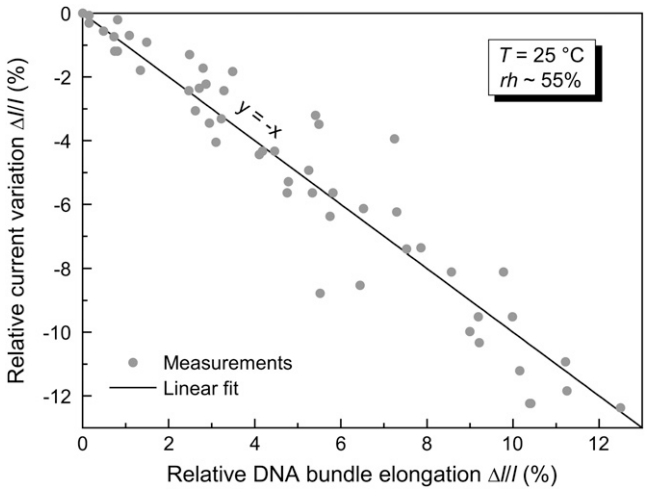

FIGURE 3 Effect of the elongation of a DNA bundle on its conductivity. The measurements were performed for a DC voltage of $U = 10$ V. The data were recorded at $T = 25$°C for $rh = 50 \sim 60\%$ (typical currents are a few tens of pA). The function $y = -x$ is a perfect match with the least-squares linear regression curve calculated over 50 measurements ($y = -1.008x$, $R^2 = 0.91$).

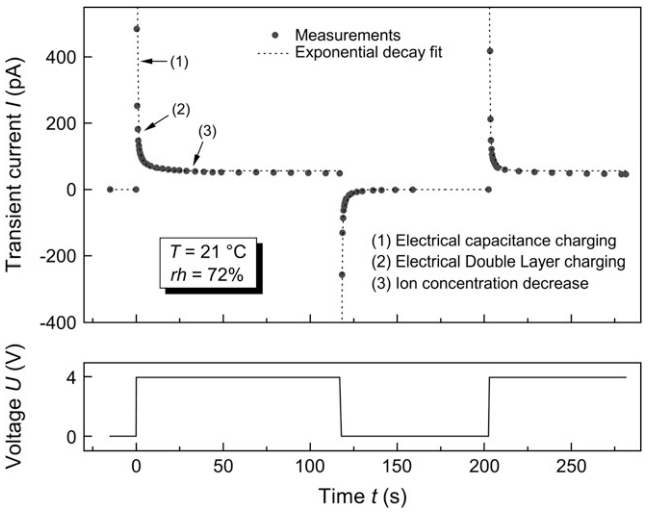

FIGURE 4 Transient current through a DNA bundle. The recording was obtained for a 4 V step (lower part of the graph). Data recorded at $T = 21$°C and $rh = 72\%$. The dotted line is an exponential decay fit with $\tau_1 = 0.3$ s, $\tau_2 = 3$ s, and $\tau_3 = \infty$.

where $S \propto \phi^2$ is the section of the bundle, and σ is its conductivity. Indeed, if σ is considered as constant for a given value of T and rh, the measurements show an Ohmic behavior as $I \propto U\phi^2/l$. The influence of humidity rh on the conductivity σ will be discussed in the following sections.

Transient current

For an applied voltage U, the current I flowing in the bundle is calculated from the Ohmic relation given in Eq. 1. Furthermore, the conductivity is described as

$$\sigma = qn\mu, \tag{2}$$

where q is the electron charge, n is the density of carriers, and μ is the carrier mobility. This model assumes that the charges q are carried by mobile ions of density n, and the kinetics of charge exchanges between ions result in a mobility μ. Putting Eqs. 1 and 2 together, we have

$$I = \frac{qn\mu SU}{l}. \tag{3}$$

In Fig. 4, we show a typical transient current measurement obtained at $rh = 72\%$ for voltage pulses of $U = 0$–4 V. We can identify three main phenomena resulting in the current decrease. As depicted in Fig. 4, we attribute the first rapid decrease of I to electrical capacitance charging in the device. The time constant ($\tau_1 \approx 0.3$ s) is typical for a stray capacitance. We also have to consider the electrical double layer (EDL) charging that takes place at the interface between the electrodes and the moisturized DNA bundle. We measured a time constant of typically $\tau_2 \approx 3$ s for the EDL formation. Finally, according to M. Watanabe et al. (38) and Nilsson (39), the long-term current decrease is due to the consumption of carriers by electrolysis. The time constant τ_3 for this phenomenon is rather large ($\tau_3 \approx 600$ s) and we assumed that $\tau_3 \gg \tau_1, \tau_2$. In such conditions, only the carrier consumption is observed after a certain time $t' \gg \tau_1, \tau_2$ and the current can be approximated by an exponential decay (38,39),

$$I(t') = \frac{SU}{l}\left((\sigma_{\text{init}} - \sigma_\infty)\exp\left(-\frac{\mu U}{l^2}t'\right) + \sigma_\infty\right), \tag{4}$$

where σ_{init} is the initial conductivity (measured at $t' = 0$), and σ_∞ is the long-term conductivity obtained when equilibrium between consumption and generation of charge carriers is reached. In Eq. 4, the current decreases with a time constant $\tau_3 = l^2/\mu U$.

The time constants τ_1, τ_2, and τ_3 have clearly different orders of magnitude. Each time constant could therefore be easily extracted from the transient measurements by considering different time periods. In Fig. 5 *a*, for clarity reasons, we only report a few of these curves and the timescale is limited to $0 \le t \le 120$ s. With such a timescale, we actually see the combined effects of τ_2 (which varies with rh) and τ_3: For lower humidity levels, due to the reduced concentration of charge carriers, the time needed to establish the EDL is longer and τ_2 is increased. This affects the slope of the curve for $t < 60$ s. For higher humidity levels, we see mainly the slope due to τ_3. The values of τ_3, which were extracted from transient measurements recorded over several minutes, did not show significant variation with rh. This indicates that the carrier mobility μ remains constant with rh since $\tau_3 = l^2/\mu U$.

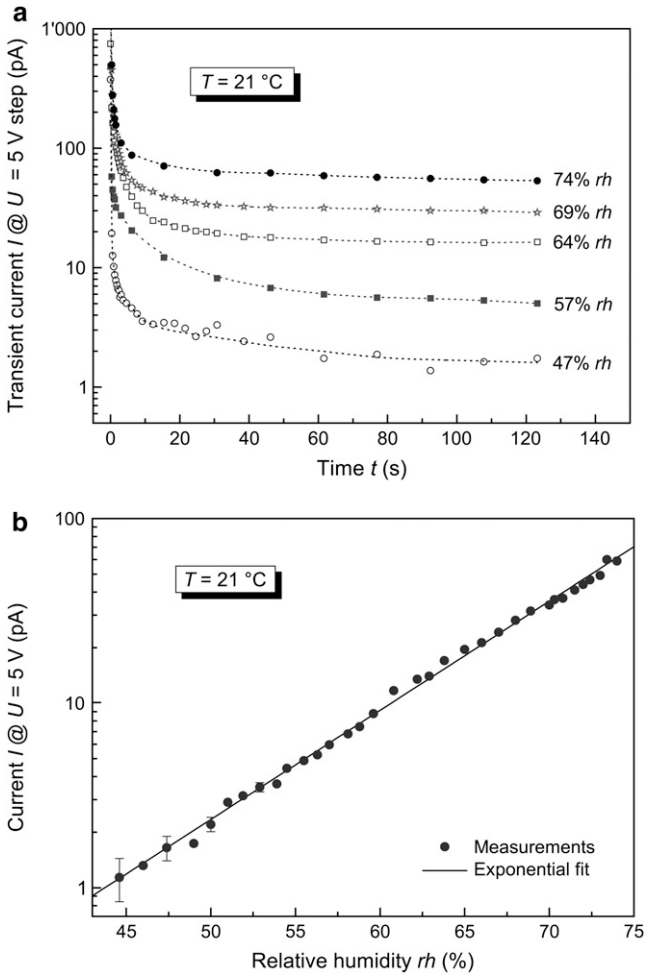

FIGURE 5 Effect of the humidity on the transient current and on the conductivity of a DNA bundle. Data recorded at $T = 21°C$ ($\pm 1°C$ overall fluctuation) for different humidity levels ($rh \pm 0.2\%$ for each curve). The relative humidity was decreased from 75% to 45% in 6 h. (*a*) Transient current through a DNA bundle for different humidity conditions. The recording were obtained for a 5 V step. The dotted lines are guides for the eye. (*b*) Exponential decrease of the current with decreasing humidity. Data extracted from the measurements of Fig. 5 *a* after $t = 60$ s. The curve is an exponential fit.

Influence of humidity

Having shown in the first section that DNA has a quasi-Ohmic behavior for constant temperature and humidity conditions, we are now interested in understanding the origin of this conductivity, that is, to know how charges propagate through the DNA bundle. It is only recently that the major influence of humidity was demonstrated (25,28). Indeed, it was shown that there is an exponential dependence of σ with *rh*. In our second set of experiments, we measured the transient current through a DNA bundle and conducted these measurements in different humidity conditions. The relative humidity was decreased slowly from 75% to 45% in 6 h, at a constant temperature $T = 21°C$. Fig. 5 *a* reports the transient current measured for different values of *rh*. The $I - rh$ curve given in Fig. 4 *b* was plotted from the data recorded in Fig. 5 *a* with the assumption that the decrease in carrier charge was always negligible. We extracted the stabilized current from Fig. 5 *a* by choosing $t' = t - 60$ s, thus considering that $\sigma_{\text{init}} = \sigma(t = 60 \text{ s})$. As previously observed by Kleine-Ostmann et al. (28), the exponential fit in Fig. 5 *b* shows that the conductivity increase is exponentially related to the relative humidity.

DISCUSSION

From the analysis of the transient measurements of $I(rh)$, we propose an explanation for the physical effect that is responsible for the electrical conductivity through DNA bundles. Equation 3 indicates that the current dependence with humidity could be due to either the increase of mobility μ or to the increase of carrier concentration n with humidity. From the experiments reported in Fig. 5 *a*, it is obvious that the mobility μ does not increase with the relative humidity *rh*, otherwise a higher mobility would result in a shorter exponential time constant τ_3. Indeed, no correlation exists between *rh* and the slopes of the curves (for $t \gg$) obtained at different humidity levels. Therefore, we can conclude that the carrier concentration n is responsible for the current increase with humidity.

Ha et al. (25) have shown that the conductivity of DNA increases exponentially with the relative humidity. Later on, Kleine-Ostmann et al. (28) have also verified this phenomenon. In both experiments, the two groups used a DNA solution spotted and dried on gold nanoelectrodes. They concluded that the current mainly flows through the water layer adsorbed on DNA. It is to be noticed that such exponential dependence with *rh* was also reported for porous oxide materials (40) and the phenomenon was used in ceramic humidity sensors based on porous oxides (41,42). In the latter case also, the exponential dependence of the conductivity was attributed to the adsorption of water molecules on the nanostructured film surfaces.

Because the current increases with humidity, it is believed that the charge carriers are the H^+ and OH^- species produced by water adsorption (25,43). The ions separate and recombine according to the Grotthus mechanism, which describes the passing of protons through the cooperation of neighboring water molecules. The dissociation reaction can be approximated at equilibrium with the dissociation constant, K (34),

$$K = \frac{[\mathrm{H}^+][\mathrm{OH}^-]}{[\mathrm{H_2O}]} = \exp\left(-\frac{\Delta G}{RT}\right), \tag{5}$$

with ΔG as the standard Gibbs energy change of reaction, R as the gas constant, and T as the absolute temperature. From the requirement of electrical neutrality, we have $[H^+] = [OH^-]$. From Eq. 5, it can be deduced that

$$[H^+] = \left([H_2O]\exp\left(-\frac{\Delta G}{RT}\right)\right)^{1/2} = \sqrt{[H_2O]}\exp\left(-\frac{\Delta G}{2RT}\right).$$

The concentration of water, $[H_2O]$, in the bundle is related to the number of water molecules adsorbed per nucleotide, N_w. According to Armitage et al. (26), N_w can be correlated to the relative humidity, *rh*, through the Brunauer-Emmett-Teller theory (44) describing the physical adsorption of gas molecules on a solid surface. From the Brunauer-Emmett-Teller equation, the adsorption of water on DNA was experimentally obtained by Armitage et al. (26):

$$N_w = \frac{44rh}{(1-rh)(1+19rh)}.$$

However, the increase of N_w with *rh* cannot explain alone the exponential dependence of the current with humidity. From their experiments on silica gel, Anderson et al. (40) suggested that the Gibbs energy provides the energy needed to overcome the Coulombic attraction. Under this consideration, we have the following relation for the conductivity:

$$\sigma \propto \sqrt{N_w}\exp\left(-\frac{q^2}{2\epsilon dRT}\right), \quad (6)$$

where *d* is the equilibrium separation distance of the charges in the neutral species ($d = 1$ Å in our model), and $\epsilon = \epsilon_r\epsilon_0$ is the permittivity. In Eq. 6, the expression $\exp(-q^2/2\epsilon dRT)$ takes into account the energy required to separate the charge species during the ion generation mechanism (25,40).

The increase of σ is mainly explained by the increase of with *rh* (40,41). Several authors have intended to model the charge transfer in the DNA-water complex and considered this system as a heterogeneous dielectric medium in which they assigned different dielectric permittivities to its different regions (45–47). In the particular case of DNA in water solution, they proposed to distinguish different dielectric zones (47): the nucleobase, the bases and sugar-phosphate backbone, the bound-water zone (3 Å thick) adjacent to the surface of the DNA fragment (ϵ_1), and the bulk water zone (ϵ_2). They also considered the bound-water zone to have reduced permittivity compared to bulk water ($\epsilon_1 < \epsilon_2$). This lowered value was attributed to the reduced motility of water molecules in the vicinity of the sugar-phosphate backbone. Also, the bound-water dielectric constant is unknown. For this reason, Siriwong et al. (47) considered various values of ϵ_1 (between 2 and 80) in their simulations. In light of these models, we consider that there is space between each DNA strand in the bundle, and that this space is definitely $\gg$3 Å. The bundle is similar to a spongy material rather than a compact assembly of DNA molecules. Under this hypothesis, it is believed that water molecules can penetrate within the bundle. This is coherent with the fact that the current varies linearly with its cross section. Indeed, this dependence shows that the conductivity does not only take place at the surface of the bundle, but comes from the contribution of each DNA strand inside the bundle. Hence, we conclude that, in our case, the global dielectric constant is a function of ϵ_1 and ϵ_2, which both depend on *rh* ($\epsilon = f(\epsilon_1, \epsilon_2, rh)$). We assumed that $\epsilon \rightarrow \epsilon_{H_2O}$ for saturated air, which is consistent with the studies cited above. Considering a linear increase of ϵ with *rh*, this model enables us to retrieve the exponential dependence of σ with *rh*. Under this hypothesis we find that if ϵ_r varies between ~60 ($rh = 10\%$) and ~75 ($rh = 90\%$), a good fit can be found between our experiments and the theoretical Eq. 6. Such values are to compare with the relative permittivity of water solution ($\epsilon_{r,H_2O} = 80$ at 20°C) and are also consistent with measured values from humidity sensor studies (35). In Fig. 6, our model is compared with the measurements of Ha et al. (25), those of Kleine-Ostmann et al. (28), and our own measurements reported in Fig. 5 *b*. In the two latter cases, the conductance is indirectly obtained through the current measured at a given voltage. As shown in Eq. 1, the current depends on the voltage but also on the length and cross section of the bundle of DNA. These parameters being different (otherwise unknown) for the three studies, a quantitative comparison is not possible. Without loss of consistency, we have thence used an arbitrary unit for the conductance.

CONCLUSION

We have designed a MEMS tool that enabled the completion of different electrical experiments on DNA bundles. We have also proposed an explanation for the electrical conductivity of DNA. We suggest that the conductivity of DNA bundles is due to water adsorption on the molecule. The exponential dependence of the conductivity with the relative

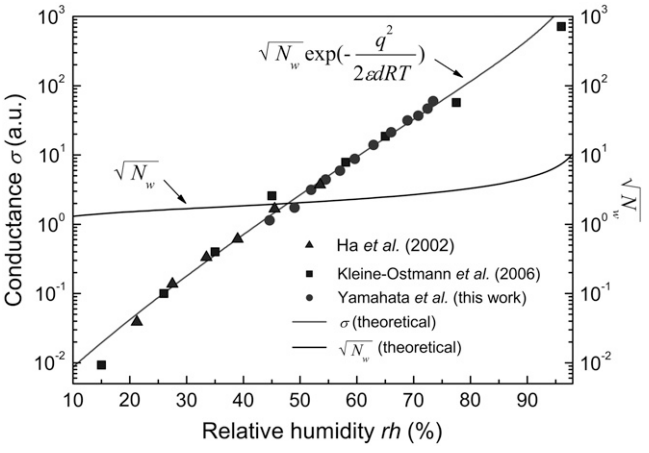

FIGURE 6 Comparison between experimental data found in the literature and the theoretical model of conductance. We plot the experimental data given in Fig. 5 *b* and fit the measurements with the model of Eq. 6. The other experimental data were extracted from the articles published by Ha et al. (25) and Kleine-Ostmann et al. (28). An arbitrary unit is used for the conductance scale because we are only interested with the slope of the curves. For comparison, we have also plotted $\sqrt{N_w}$: It clearly shows that the increase of ϵ with *rh*, rather than that of adsorbed water (N_w), is the dominating parameter that explains the increase of σ.

humidity can then be explained by the change of permittivity arising from this adsorption. Our results showing the influence of relative humidity are comparable with those obtained by Ha et al. (25) and Kleine-Ostmann et al. (28). The global model that we have formulated to describe the physical phenomenon responsible for the conductivity of DNA can also be compared to different studies that were conducted on other materials subjected to varying humidity conditions.

The photolithography masks were fabricated with the 8-inch EB writer F5112+VD01 donated by Advantest Corporation to the VLSI Design and Education Center (VDEC, the University of Tokyo).

This work was supported by the Swiss National Science Foundation (grant No. PBEL2–107898), the Japan Society for the Promotion of Science (grant No. P06373), and a grant for Advanced Instrumentation (''Development of Handling and Characterization Tools for Nano Objects'') from the Japan Science and Technology Corporation.

REFERENCES

1. Rothemund, P. W. K., N. Papadakis, and E. Winfree. 2004. Algorithmic self-assembly of DNA Sierpinski triangles. *PLoS Biol.* 2:2041–2053.
2. Tanaka, K., G. H. Clever, Y. Takezawa, Y. Yamada, C. Kaul, M. Shionoya, and T. Carell. 2006. Programmable self-assembly of metal ions inside artificial DNA duplexes. *Nature Nanotechnol.* 1:190–194.
3. Bustamante, C., Z. Bryant, and S. B. Smith. 2003. Ten years of tension: single-molecule DNA mechanics. *Nature.* 421:423–427.
4. Collard, D., C. Yamahata, B. Legrand, T. Takekawa, M. Kumemura, N. Sakaki, G. Hashiguchi, and H. Fujita. 2007. Towards mechanical characterization of biomolecules by MNEMS tools. *IEEJ Trans. Electr. Electron. Eng.* 2:262–271.
5. Strick, T. R., V. Croquette, and D. Bensimon. 2000. Single-molecule analysis of DNA uncoiling by a type II topoisomerase. *Nature.* 404: 901–904.
6. Porath, D., N. Lapidot, and J. Gomez-Herrero. 2006. Charge transport in DNA-based devices. *In* Introducing Molecular Electronics, Vol. 680, Lecture Notes in Physics. Springer, Berlin, Heidelberg. 411–444.
7. Boon, E. M., and J. K. Barton. 2002. Charge transport in DNA. *Curr. Opin. Struct. Biol.* 12:320–329.
8. Endres, R. G., D. L. Cox, and R. R. P. Singh. 2004. Colloquium: The quest for high-conductance DNA. *Rev. Mod. Phys.* 76:195–214.
9. Fink, H. W., and C. Schönenberger. 1999. Electrical conduction through DNA molecules. *Nature.* 398:407–410.
10. Porath, D., A. Bezryadin, S. de Vries, and C. Dekker. 2000. Direct measurement of electrical transport through DNA molecules. *Nature.* 403:635–638.
11. Watanabe, H., C. Manabe, T. Shigematsu, K. Shimotani, and M. Shimizu. 2001. Single molecule DNA device measured with triple-probe atomic force microscope. *Appl. Phys. Lett.* 79:2462–2464.
12. Cohen, H., C. Nogues, R. Naaman, and D. Porath. 2005. Direct measurement of electrical transport through single DNA molecules of complex sequence. *Proc. Natl. Acad. Sci. USA.* 102:11589–11593.
13. Cai, L. T., H. Tabata, and T. Kawai. 2000. Self-assembled DNA networks and their electrical conductivity. *Appl. Phys. Lett.* 77:3105–3106.
14. Cai, L. T., H. Tabata, and T. Kawai. 2001. Probing electrical properties of oriented DNA by conducting atomic force microscopy. *Nanotechnology.* 12:211–216.
15. Yoo, K. H., D. H. Ha, J. O. Lee, J. W. Park, J. Kim, J. J. Kim, H. Y. Lee, T. Kawai, and H. Y. Choi. 2001. Electrical conduction through poly(dA)-poly(dT) and poly(dG)-poly(dC) DNA molecules. *Phys. Rev. Lett.* 87:198102/1–198102/4.
16. Xu, B. Q., P. M. Zhang, X. L. Li, and N. J. Tao. 2004. Direct conductance measurement of single DNA molecules in aqueous solution. *Nano Lett.* 4:1105–1108.
17. Iqbal, S. M., G. Balasundaram, S. Ghosh, D. E. Bergstrom, and R. Bashir. 2005. Direct current electrical characterization of ds-DNA in nanogap junctions. *Appl. Phys. Lett.* 86:153901/1–153901/3.
18. Rakitin, A., P. Aich, C. Papadopoulos, Y. Kobzar, A. S. Vedeneev, J. S. Lee, and J. M. Xu. 2001. Metallic conduction through engineered DNA: DNA nanoelectronic building blocks. *Phys. Rev. Lett.* 86:3670–3673.
19. Tabata, H., L. T. Cai, J. H. Gu, S. Tanaka, Y. Otsuka, Y. Sacho, M. Taniguchi, and T. Kawai. 2003. Toward the DNA electronics. *Synth. Metals.* 133:469–472.
20. Maruccio, G., P. Visconti, V. Arima, S. D'Amico, A. Blasco, E. D'Amone, R. Cingolani, R. Rinaldi, S. Masiero, T. Giorgi, and G. Gottarelli. 2003. Field effect transistor based on a modified DNA base. *Nano Lett.* 3:479–483.
21. Hosogi, M., G. Hashiguchi, M. Haga, T. Yonezawa, K. Kakushima, and H. Fujita. 2005. Electrical conductivity of λDNA-Pd wire. *Jap. J. Appl. Phys. 2 Lett. Express Lett.* 44:L955–L957.
22. Müller, J. 2006. Chemistry: metals line up for DNA. *Nature.* 444:698.
23. Lee, J. M., S. K. Ahn, K. S. Kim, Y. Lee, and Y. Roh. 2006. Comparison of electrical properties of M- and λ-DNA attached on the Au metal electrodes with nanogap. *Thin Solid Films.* 515:818–821.
24. Tran, P., B. Alavi, and G. Gruner. 2000. Charge transport along the λ-DNA double helix. *Phys. Rev. Lett.* 85:1564–1567.
25. Ha, D. H., H. Nham, K. H. Yoo, H. M. So, H. Y. Lee, and T. Kawai. 2002. Humidity effects on the conductance of the assembly of DNA molecules. *Chem. Phys. Lett.* 355:405–409.
26. Armitage, N. P., M. Briman, and G. Grüner. 2004. Charge transfer and charge transport on the double helix. *Phys. Stat. Sol. (B).* 241:69–75.
27. Tuukkanen, S., A. Kuzyk, J. J. Toppari, V. P. Hytönen, T. Ihalainen, and P. Törmä. 2005. Dielectrophoresis of nanoscale double-stranded DNA and humidity effects on its electrical conductivity. *Appl. Phys. Lett.* 87:183102/1–183102/3.
28. Kleine-Ostmann, T., C. Jördens, K. Baaske, T. Weimann, M. H. de Angelis, and M. Koch. 2006. Conductivity of single-stranded and double-stranded deoxyribose nucleic acid under ambient conditions: the dominance of water. *Appl. Phys. Lett.* 88:102102/1–102102/3.
29. Hashiguchi, G., T. Goda, M. Hosogi, K. Hirano, N. Kaji, Y. Baba, K. Kakushima, and H. Fujita. 2003. DNA manipulation and retrieval from an aqueous solution with micromachined nanotweezers. *Anal. Chem.* 75:4347–4350.
30. Yamahata, C., T. Takekawa, K. Ayano, M. Hosogi, M. Kumemura, B. Legrand, D. Collard, G. Hashiguchi, and H. Fujita. 2006. Silicon nanotweezers with adjustable and controllable gap for the manipulation and characterization of DNA molecules. *In* Proceedings of the IEEE International Conference on Microtechnologies in Medicine and Biology. Okinawa, Japan.
31. Yamahata, C., T. Takekawa, M. Kumemura, M. Hosogi, G. Hashiguchi, D. Collard, and H. Fujita. 2007. Electrical and mechanical characteristics of DNA bundles revealed by silicon nanotweezers. *In* Technical Digest of Transducers '07, the 14th International Conference on Solid-State Sensors, Actuators and Microsystems, Vol. 1. Lyon, France.
32. Washizu, M., O. Kurosawa, I. Arai, S. Suzuki, and N. Shimamoto. 1995. Applications of electrostatic stretch-and-positioning of DNA. *IEEE Trans. Ind. Appl.* 31:447–456.
33. Yamamoto, T., O. Kurosawa, H. Kabata, N. Shimamoto, and M. Washizu. 2000. Molecular surgery of DNA based on electrostatic micromanipulation. *IEEE Trans. Ind. Appl.* 36:1010–1017.
34. Kumemura, M., D. Collard, C. Yamahata, N. Sakaki, G. Hashiguchi, and H. Fujita. 2007. Single DNA molecule isolation and trapping in a microfluidic device. *ChemPhysChem.* 8:1875–1880.

35. Ueda, M., Y. Baba, H. Iwasaki, O. Kurosawa, and M. Washizu. 1999. Direct observation of deoxyribonucleic acid anchored between an aluminum electrode and an atomic force microscope cantilever. *Jap. J. Appl. Phys. 1 Reg. Papers. Short Notes Rev. Papers.* 38: 6568–6569.

36. Wu, J., F. Du, P. Zhang, I. A. Khan, J. Chen, and Y. Liang. 2005. Thermodynamics of the interaction of aluminum ions with DNA: implications for the biological function of aluminum. *J. Inorg. Biochem.* 99:1145–1154.

37. Wang, J., and A. J. Bard. 2001. Monitoring DNA immobilization and hybridization on surfaces by atomic force microscopy force measurements. *Anal. Chem.* 73:2207–2212.

38. Watanabe, M., M. Rikukawa, K. Sanui, and N. Ogata. 1985. Evaluation of ionic mobility and transference number in a polymeric solid electrolyte by isothermal transient ionic current method. *J. Appl. Phys.* 58:736–740.

39. Nilsson, M. 2006. Conductance phenomena in microcrystalline cellulose. *Phys. Stat. Sol.* (*C*). 3:251–254.

40. Anderson, J. H., and G. A. Parks. 1968. Electrical conductivity of silica gel in presence of adsorbed water. *J. Phys. Chem.* 72:3662–3668.

41. Yeh, Y. C., and T. Y. Tseng. 1989. Analysis of the DC and AC properties of K_2O-doped porous $Ba_{0.5}Sr_{0.5}TiO_3$ ceramic humidity sensor. *J. Mater. Sci.* 24:2739–2745.

42. Tai, W.-P., J.-G. Kim, J.-H. Oh, C. Lee, D.-W. Park, and W.-S. Ahn. 2005. Humidity sensing properties of nanostructured-bilayered potassium tantalate: Titania films. *J. Mater. Sci. Mater. Electron.* 16:517–521.

43. Tuckerman, M. E., D. Marx, and M. Parrinello. 2002. The nature and transport mechanism of hydrated hydroxide ions in aqueous solution. *Nature.* 417:925–929.

44. Brunauer, S., P. H. Emmett, and E. Teller. 1938. Adsorption of gases in multimolecular layers. *J. Am. Chem. Soc.* 60:309–319.

45. Yang, L. Q., S. Weerasinghe, P. E. Smith, and B. M. Pettitt. 1995. Dielectric response of triplex DNA in ionic solution from simulations. *Biophys. J.* 69:1519–1527.

46. Tavernier, H., and M. Fayer. 2000. Distance dependence of electron transfer in DNA: the role of the reorganization energy and free energy. *J. Phys. Chem. B.* 104:11541–11550.

47. Siriwong, K., A. A. Voityuk, M. D. Newton, and N. Rösch. 2003. Estimate of the reorganization energy for charge transfer in DNA. *J. Phys. Chem. B.* 107:2595–2601.